Recombinant production of *Yersinia enterocolitica* pyruvate kinase isoenzymes PykA and PykF

Julia Hofmann[1], Christine Heider[1], Wei Li[2], Joern Krausze[2], Manfred Roessle[3,4], and Gottfried Wilharm[1,*]

[1] Robert Koch-Institute, Wernigerode Branch, Burgstr. 37, D-38855 Wernigerode, Germany

[2]Department of Molecular Structural Biology, Helmholtz Centre for Infection Research, D-38124 Braunschweig, Germany

[3] European Molecular Biology Laboratory, Hamburg Outstation, c/o DESY, Notkestrasse 85, D-22603 Hamburg, Germany

[4]present address: Luebeck University of Applied Science; Moenkhoferweg 239, 23562 Luebeck

*Address correspondence to: Gottfried Wilharm, Robert Koch-Institut, Bereich Wernigerode, Burgstr. 37, D-38855 Wernigerode, Germany; Phone: +49 3943 679 282; Fax: +49 3943 679 207;

E-mail: wilharmg@rki.de

Running title: *Yersinia enterocolitica* pyruvate kinases PykA and PykF

Abstract

The glycolytic enzyme pyruvate kinase (PK) generates ATP from ADP through substrate-level phosphorylation powered by the conversion of phosphoenolpyruvate to pyruvate. In contrast to other bacteria, *Enterobacteriaceae*, such as pathogenic yersiniae, harbour two pyruvate kinases encoded by *pykA* and *pykF*. The individual roles of these isoenzymes are poorly understood. In an attempt to make the *Yersinia enterocolitica* pyruvate kinases PykA and PykF amenable to structural and functional characterization, we produced them untagged in *E. coli* and purified them to near homogeneity through a combination of ion exchange and size exclusion chromatography, yielding more than 180 milligram per litre of batch culture. The solution structure of PykA and PykF was analysed through small angle X-ray scattering which revealed the formation of PykA and PykF tetramers and confirmed the binding of the allosteric effector fructose-1,6-bisphosphate (FBP) to PykF but not to PykA.

Keywords

Yersinia enterocolitica – pyruvate kinase – PykA – PykF – *E. coli* – recombinant

Highlights

- High-level expression and purification of *Yersinia enterocolitica* pyruvate kinase isoenzymes PykA and PykF
- Efficient two-step purification without any affinity tag
- Formation of PykA and PykF tetramers confirmed by SAXS

Introduction

Pyruvate kinase (PK) catalyses the last step in glycolysis enabling substrate-level phosphorylation to form ATP from ADP on the expenditure of phosphoenolpyruvate which is converted to pyruvate. Within the last years, research on PK enzymes experienced a significant boost as it became more and more evident that these enzymes play a crucial role in tumor biology and therefore represent potential drug targets [1]. Furthermore, interest in bacterial and parasites' PK enzymes has developed in search of potential drug target molecules [2-5]. While four PK isoenzymes are known in mammalians, bacteria typically harbour a single PK enzyme. However, a few bacteria harbour two PK isoenzymes, especially members of the *Enterobacteriaceae* such as *E. coli*, *Salmonella* and *Yersinia*. The type I PK (PykF) of *E. coli* is characterised as an enzyme that is allosterically activated by FBP, whereas type II PK (PykA) is not [6, 7]. The two PK types are phylogenetically distant and share a sequence identity of only 37% in *E. coli* and of 39% identity in *Y. enterocolitica*. While PykF crystal structures are available and show the tetrameric organisation typical of PK enzymes [8, 9], structural data on PykA homologues are missing. In activity assays, PykF significantly surpasses PykA activity under all conditions tested [6, 10, 11] leaving open the question of why these bacteria need two isoenzymes. In *E. coli*, the deletion of both *pyk* genes increases expression and activity of phosphoenolpyruvate carboxylase (PEPC), a fact that indicates the rerouting of carbon fluxes via PEPC [12]. Similarly, deletion of the *pykF* gene alone also stimulated PEPC expression and activity, which suggested a low-level residual PK activity mediated by PykA [11].

Recently, our attention was drawn to pyruvate kinases of pathogenic *Yersinia* as we identified an interrelationship between their type three secretion system (T3SS) and central carbon metabolism [13]. The *Yersinia* T3SS is supposed to form a molecular microinjection device dedicated to the manipulation of host cells by injection of effector proteins [14].

Regulatory components of the *Yersinia enterocolitica* T3SS, YscM1 and YscM2, were found to physically interact with *Yersinia* PEPC, and metabolic flux analyses furthermore suggested a role of PK in this regulatory network of virulence and metabolic functions [13].

Given that many of the few bacteria harbouring two PK isoenzymes are pathogens, understanding their particular roles may contribute to our understanding of virulence.

The PK isoenzymes PykA and PykF of *Yersinia* have not been studied to date. Here, we report on the highly efficient large-scale recombinant production of both isoenzymes, making them amenable to structural and functional characterisation.

Materials and methods

Construction of expression plasmids

Pyruvate kinase encoding genes *pykA* and *pykF* of *Y. enterocolitica* WA-314 were amplified by PCR as follows and inserted into IPTG-inducible expression vector pWS [15]. To amplify *pykA* by PCR the following oligonucleotides were used: pykA_NdeI_for (5'-AATGACATATGTCCAGACGGCTTAGAAGGAC-3') and pykA_BglII_rev (5'-CACATAGATCTTCATTCAACACGCAGAATGCGGC-3'), while for amplification of *pykF* the primers pykF_NdeI_for (5'-AATGACATATGAAAAAGACTAAAATTGTTTGTACTATCG-3') and pykF_SalI_rev (5'-CACAGGTCGACTTATAAAACGTGCACGGAAGAGGTATTGG-3') were used. Underlined letters in the primer sequences indicate restriction enzyme recognition sites introduced for subsequent ligation into expression vector pWS. The resulting plasmids (pWS-*pykA* and pWS-*pykF*) were confirmed by DNA sequencing and were transformed into expression strain *E. coli* BL21 (DE3) pLysS.

Protein expression and purification

Overnight cultures of *E. coli* BL21 (DE3) pLysS pWS-*pykA* and *E. coli* BL21 (DE3) pLysS pWS-*pykF***,** respectively, were grown in 2YT medium (16 g/L tryptone, 5 g/L yeast extract, 5 g/L NaCl) at 37°C, diluted 1:50 into 400 mL of 2YT and cultured in a 2L-flask at 37°C and 150 rpm until OD_{600nm} reached a value of 0.6. Expression was induced by addition of 0.1 mM IPTG and cultures were incubated for 5 hours at 27°C. Cells were harvested by centrifugation and pellets frozen at -80°C. Cell pellets were solubilised at 4°C in 10 mM Tris pH 8.5, 50 mM KCl, 5 mM DTT at a ratio of 7 mL of buffer per gram of cell paste. The solubilization buffer was supplemented with Complete Protease Inhibitor Cocktail (Roche Diagnostics GmbH). Cells were lysed applying three passages through an EmulsiFlex-C3 homogeniser (Avestin). Lysates were cleared by centrifugation at 20.000 g for 20 min and subsequent passage through 0.2 µm sterile filters (Sartorius, Germany).

Ion exchange chromatography: A HiPrep 16/10 Q XL column (GE Healthcare) was equilibrated with 5 column volumes (CV) of buffer A (10 mM Tris pH 8.5, 50 mM KCl, 1 mM DTT). After loading of the soluble lysate the column was washed with 10 CV (~200 ml) of buffer A and subsequently eluted with 20 CV in a linear gradient from 0% to 25% of buffer B (10 mM Tris pH 8.5, 1 M KCl, 1 mM DTT). Loading, washing and elution were performed at a flow rate of 1 ml/min. Eluates were fractionated and examined by SDS-PAGE. PykA (pI 6.8) eluted in the range of 130-185 mM KCl and PykF (pI 6) eluted in the range of 160-200 mM KCl. The protein content of the fractions was analysed through SDS-PAGE and appropriate fractions were pooled and concentrated prior to gel filtration using polyethersulfone (PES) membranes (Sartorius Stedim Biotech, Vivaspin 20) with a molecular weight cut-off of 30 kD.

Size exclusion chromatography: A HiLoad 26/60 Superdex 200 prep grade column (GE Healthcare) equilibrated with buffer C (10 mM Tris pH 8, 100 mM KCl, 1 mM DTT) was loaded with the concentrated protein (maximum volume of 12.5 mL). The elution was carried out with the same buffer applying one CV (~330 ml) at a flow rate of 2 ml/min. The fractions were analysed by SDS-PAGE, pooled accordingly and concentrated. PykA (51.5 kDa) eluted with a maximum at 177 ml, whereas PykF (50.5 kDa) eluted slightly earlier with a maximum at 171 ml. The Superdex 200 prep grade column was calibrated with protein standards purchased from Sigma (Germany) to estimate molecular masses of PK complexes.

Pyruvate kinase (PK) activity assay

To measure PK activity, the reaction catalysed by PK was coupled with the lactate dehydrogenase (LDH) reaction. While LDH converts pyruvate to lactate it oxidises NADH to NAD^+. The concentration of the latter was then measured at 340 nm [16]. The reaction mixture consisted of 50 mM Tris pH 7.5, 100 mM KCl, 10 mM $MgCl_2$, 2.5 mM NADH, 2.4 U LDH , 2 mM ADP, 5 mM PEP, and 100 nM of PykA and PykF, respectively. Reaction mixtures without PEP were pre-incubated for 5 min at 30°C, then reactions were started by addition of PEP. Reactions of 100 µl were recorded for 1 minute at 30°C with a Specord 50 photometer (Analytik Jena, Germany) and the slopes of triplicates were averaged for calculation of NADH oxidation and PK activity, respectively. One unit of PK activity corresponds to 1 µmol of oxidized NADH per minute.

Protein quantitation

Protein concentrations were determined applying the modified Bradford assay purchased from Bio-Rad (Germany) and using BSA as a standard. Protein gels were analyzed using the ImageJ software package.

Circular dichroism (CD) spectroscopy

CD data were acquired on a Jasco J-815 CD spectrometer (Jasco, Inc). PykA (22 μM), PykF (10 μM), and PykF in the presence of fructose-1,6-bisphosphate (FBP) (10 mM) were equilibrated in 20mM Tris-HCl (pH 8.0) and measured at 10 °C in 0.1-cm path length cuvette. Spectra were recorded in the 190-260 nm wavelength range with 1 nm increments (20 nm / min), 10 s averaging time, and 1 nm bandwidth for 10 repeats. The mean residue molar ellipticity was calculated by

$$[\Theta] = \Theta \times 100 \times M / C \times l \times n$$

where Θ is the ellipticity in degrees, l the optical path in cm, C the protein concentration in mg/ml, M is the protein's molecular mass, n the number of residues in the protein, and $[\Theta]$ the mean residue molar ellipticity in deg•cm^2•dmol^{-1}. The baseline-corrected spectra were used for protein secondary structure analysis.

Small angle X-ray scattering (SAXS)

The synchrotron radiation X-ray scattering data were collected following standard procedures on the X33 SAXS camera of the EMBL Hamburg located on a bending magnet (sector D) on the storage ring DORIS III of the Deutsches Elektronen Synchrotron (DESY) [17, 18]. As detector, a single photon counting pixel detector (PILATUS 1M, Dectris, Villingen, Switzerland) was used. A sample - detector distance of 3400 mm was used, covering the range of momentum transfer $0.11 < s < 2.8$ nm^{-1} ($s = 4\pi \sin(\theta)/\lambda$, where θ is the

scattering angle and λ = 0.1504 nm is the X-ray wavelength) [18]. The S-axis was calibrated by the scattering pattern of Silver-behenate salt (d-spacing 5.84 nm). The protein solutions were automatically loaded to the vacuum sample chamber by a liquid handling sample changer robot [18, 19]. The scattering patterns from PykA, PykF, and PykF with FBP were measured at different protein concentrations in order to check for interparticle interferences. Protein samples were prepared in 10 mM Tris pH 8, 100 mM KCl and 1 mM DTT as radical quencher. Repetitive measurements of 15 sec at 10 °C of the same protein solution were performed in order to check for radiation damage. Stable intensities especially at low angles indicated that no protein aggregation took place during the exposure times. The data were normalized to the intensity of the incident beam; the scattering of the buffer was subtracted and the difference curves were scaled for concentration. All the data processing steps were performed using the program package PRIMUS [20]. The forward scattering *I(0)* and the radius of gyration R_g were evaluated using the Guinier approximation [21] assuming that for spherical particles at very small angles ($s < 1.3/R_g$) the intensity is represented by $I(s) = I(0) \exp(-(sR_g)^2/3)$. These parameters were also computed from the entire scattering patterns using the indirect transform package GNOM [22], which also provide the distance distribution function *p(r)* of the particle as defined:

$$p(r)=2\pi\int I(s)sr\sin(sr)ds$$

The molecular masses of PykA, PykF and PykF with FBP were calculated by comparison with the forward scattering from the reference solution of bovine serum albumin (BSA). From this procedure a relative calibration factor for the molecular mass (MM) can be calculated using the known molecular mass of BSA (66 kDa) and the concentration of the reference solution by applying

$$MM_p = I(0)_p / c_p \times \frac{MM_{st}}{I(0)_{st} / c_{st}}$$

where $I(0)_p$, $I(0)_{st}$ are the scattering intensities at zero angle of the studied and the BSA standard protein, respectively, MM_p, MM_{st} are the corresponding molecular masses and c_p, c_{st} are the concentrations. Errors on molecular weights have been calculated from the upper and the lower I(0) error limit estimated by the Guinier approximation.

Low-resolution models of PykA, PykF, and PykF with FBP were built by the program DAMMIN [23], which represents the protein as an assembly of dummy atoms inside a search volume defined by a sphere of the diameter D_{max}. Starting from a random model, DAMMIN employs simulated annealing to build a scattering equivalent model fitting the experimental data $I_{exp}(s)$ to minimize discrepancy:

$$\chi^2 = \frac{1}{N-1}\sum_j \left[\frac{I_{\exp}(s_j) - cI_{calc}(s_j)}{\sigma(s_j)}\right]^2$$

where N is the number of experimental points, c a scaling factor and $I_{calc}(s_j)$ and $\sigma(s_j)$ are the calculated intensity and the experimental error at the momentum transfer s_j, respectively. *Ab initio* shape models for PykA, PykF and PykF with FBP respectively were obtained by superposition of 20 independent DAMMIN reconstructions for each subunit by using the program packages DAMAVER [23] and SUBCOMP [23].

Results and discussion

To recombinantly produce *Yersinia enterocolitica* pyruvate kinases PykA and PykF in their outright form without any tag, *pykA* and *pykF* coding regions were amplified by PCR and cloned into IPTG-inducible expression vector pWS [15]. Using BL21 pLysS as expression host, solubility of both PykA and PykF was superior when expression cultures were incubated at 27°C compared to 37°C, so that for large-scale production both proteins were expressed at 27°C after induction for 5 hours. In an analogous manner, both proteins

were purified from 400 ml of expression culture, applying ion exchange chromatography on a HiPrep 16/10 Q XL column and a subsequent size exclusion chromatography step on a Superdex 200 prep grade column. The purification of PykA and PykF is summarized in Tables 1 and 2 and illustrated by Figure 1, showing representative samples of both purification procedures analysed on Coomassie-stained gels after SDS-PAGE. The yield was approx. 100 and 73 mg of PykA and PykF, respectively, per 400 ml of expression culture corresponding to 250 and 183 mg/L. To the best of our knowledge, this is superior to any other reported PK expression and purification protocol (see Table 3). The specific activities determined for purified *Y. enterocolitica* PykA and PykF (85 and 108 U/mg) are in good agreement with values determined for other bacterial PK enzymes [24] (see Table 3). Elution of PykA and PykF from preparative size exclusion chromatography was in accordance with formation of tetramers (data not shown). Interestingly PykF (calculated monomeric mass of 50.5 kDa) eluted significantly and reproducibly before PykA (51.5 kDa) with a peak maximum at 171 mL for PykF compared to 177 mL for PykA (data not shown). This could be explained by an unspecific interaction of PykA with the gel matrix delaying elution. Alternatively, a significant difference in the conformation of the PykA and the PykF tetramers such as induced by stable binding of a low molecular weight ligand (e.g. an allosteric effector) could be the reason for this phenomenon. The CD spectra (Fig. 2) exhibited two minima around 208 nm and 222 nm, which is a typical indication of α-helix conformation. Recorded CD spectra illustrate considerable structural differences between PykA and PykF and confirm their overall high content of α-helices. In the presence of the known allosteric activator fructose-1,6-bisphosphate (FBP) the CD spectrum of PykF was only marginally changed.

To confirm the tetrameric organization of the purified isoenzymes, small angle X-ray scattering (SAXS) was applied (Fig. 3; supplementary data 1). Both, PykA and PykF formed tetramers, which were distinct (Fig. 3A and B). This could explain their significantly differing elution behaviour on the Superdex 200 column. Furthermore, a conformational transition of

the PykF tetramer could be observed upon addition of the allosteric effector fructose-1,6-bisphosphate (FBP) (Fig. 3B and C). The allosteric activation of PykF-like PK enzymes is well-known, but to our knowledge the conformational transition has never been demonstrated applying SAXS. No conformational transition of PykA in the presence of FBP could be observed (data not shown), which is in line with the lack of allosteric influence of FBP on PykA-like enzymes [24].

Interestingly, available crystal structure coordinates of *E. coli* PykF (PDB: 1pky), being 86% identical to *Y. enterocolitica* PykF, did not fit very well into the SAXS-based model (data not shown). This could indicate differences between solution structure and crystal packing, or, alternatively, this could indicate differences between the homologous enzymes of *E. coli* and *Y. enterocolitica*.

Finally, it is worthwhile mentioning that initially we had expressed PykA and PykF as glutathione S-transferase (GST) fusion proteins using plasmid pGEX-4T3 and yielded high level expression and purification of GST-PykA and GST-PykF. However, we failed to cleave both fusion proteins efficiently using thrombin, possibly due to steric hindrance.

Collectively, the high-level production of *Y. enterocolitica* PykA and PykF may pave the way for their structural and functional characterization. In addition, this study highlights the use of SAXS to study allosteric transition states of pyruvate kinases.

Acknowledgements

We thank members of the sequencing core facility at the Robert Koch-Institute for DNA sequencing. This work was supported by a grant from the Deutsche Forschungsgemeinschaft (SPP 1316; WI 3272/1-1 and WI 3272/1-2).

References

[1] S. Mazurek, Pyruvate kinase M2: A key enzyme of the tumor metabolome and its medical relevance. Biomedical Research (Aligarh) 23 (2012).

[2] P. Axerio-Cilies, R.H. See, R. Zoraghi, L. Worral, T. Lian, N. Stoynov, J. Jiang, S. Kaur, L. Jackson, H. Gong, Cheminformatics-Driven Discovery of Selective, Nanomolar Inhibitors for Staphylococcal Pyruvate Kinase. ACS chemical biology 7 (2011) 350-359.

[3] B.C.L. Chan, M. Ip, C. Lau, S.L. Lui, C. Jolivalt, C. Ganem-Elbaz, M. Litaudon, N.E. Reiner, H. Gong, R.H. See, Synergistic effects of baicalein with ciprofloxacin against NorA over-expressed methicillin-resistant *Staphylococcus aureus* (MRSA) and inhibition of MRSA pyruvate kinase. Journal of ethnopharmacology 137 (2011) 767-773.

[4] M. Chan, D.S.H. Tan, T. Sim, *Plasmodium falciparum* pyruvate kinase as a novel target for antimalarial drug-screening. Travel medicine and infectious disease 5 (2007) 125-131.

[5] R. Zoraghi, R.H. See, P. Axerio-Cilies, N.S. Kumar, H. Gong, A. Moreau, M. Hsing, S. Kaur, R.D. Swayze, L. Worrall, E. Amandoron, T. Lian, L. Jackson, J. Jiang, L. Thorson, C. Labriere, L. Foster, R.C. Brunham, W.R. McMaster, B.B. Finlay, N.C. Strynadka, A. Cherkasov, R.N. Young, N.E. Reiner, Identification of pyruvate kinase in methicillin-resistant *Staphylococcus aureus* as a novel antimicrobial drug target. Antimicrobial agents and chemotherapy 55 (2011) 2042-2053.

[6] A. Garrido-Pertierra, R.A. Cooper, Evidence for two dinstinct pyruvate kinase genes in *Escherichia coli* K-12. FEBS letters 162 (1983) 420-422.

[7] E.B. Waygood, B.D. Sanwal, The control of pyruvate kinases of *Escherichia coli*. I. Physicochemical and regulatory properties of the enzyme activated by fructose 1,6-diphosphate. The Journal of biological chemistry 249 (1974) 265-274.

[8] A. Mattevi, G. Valentini, M. Rizzi, M.L. Speranza, M. Bolognesi, A. Coda, Crystal structure of *Escherichia coli* pyruvate kinase type I: molecular basis of the allosteric transition. Structure (London, England: 1993) 3 (1995) 729.

[9] G. Valentini, L. Chiarelli, R. Fortin, M.L. Speranza, A. Galizzi, A. Mattevi, The allosteric regulation of pyruvate kinase. Journal of Biological Chemistry 275 (2000) 18145-18152.

[10] E. Ponce, N. Flores, A. Martinez, F. Valle, F. Bolívar, Cloning of the two pyruvate kinase isoenzyme structural genes from *Escherichia coli*: the relative roles of these enzymes in pyruvate biosynthesis. Journal of bacteriology 177 (1995) 5719-5722.

[11] K.A.Z. Siddiquee, M.J. Arauzo-Bravo, K. Shimizu, Effect of a pyruvate kinase (pykF-gene) knockout mutation on the control of gene expression and metabolic fluxes in Escherichia coli. FEMS microbiology letters 235 (2004) 25-33.

[12] M. Emmerling, M. Dauner, A. Ponti, J. Fiaux, M. Hochuli, T. Szyperski, K. Wüthrich, J. Bailey, U. Sauer, Metabolic flux responses to pyruvate kinase knockout in *Escherichia coli*. Journal of bacteriology 184 (2002) 152-164.

[13] A. Schmid, W. Neumayer, K. Trülzsch, L. Israel, A. Imhof, M. Roessle, G. Sauer, S. Richter, S. Lauw, E. Eylert, Cross-talk between type three secretion system and metabolism in *Yersinia*. Journal of Biological Chemistry 284 (2009) 12165-12177.

[14] G.R. Cornelis, The yersinia ysc-yoptype III'weaponry. Nature Reviews Molecular Cell Biology 3 (2002) 742-754.

[15] M. Locher, B. Lehnert, K. Krauss, J. Heesemann, M. Groll, G. Wilharm, Crystal structure of the *Yersinia enterocolitica* type III secretion chaperone SycT. Journal of Biological Chemistry 280 (2005) 31149-31155.

[16] T. Bücher, G. Pfleiderer, [66] Pyruvate kinase from muscle: Pyruvate phosphokinase, pyruvic phosphoferase, phosphopyruvate transphosphorylase, phosphate—transferring

enzyme II, etc. Phosphoenolpyruvate+ ADP⇌ Pyruvate+ ATP. Methods in enzymology 1 (1955) 435-440.

[17] M.W. Roessle, R. Klaering, U. Ristau, B. Robrahn, D. Jahn, T. Gehrmann, P. Konarev, A. Round, S. Fiedler, C. Hermes, Upgrade of the small-angle X-ray scattering beamline X33 at the European Molecular Biology Laboratory, Hamburg. Journal of Applied Crystallography 40 (2007) s190-s194.

[18] A. Round, D. Franke, S. Moritz, R. Huchler, M. Fritsche, D. Malthan, R. Klaering, D. Svergun, M. Roessle, Automated sample-changing robot for solution scattering experiments at the EMBL Hamburg SAXS station X33. Journal of Applied Crystallography 41 (2008) 913-917.

[19] C.E. Blanchet, A.V. Zozulya, A.G. Kikhney, D. Franke, P.V. Konarev, W. Shang, R. Klaering, B. Robrahn, C. Hermes, F. Cipriani, Instrumental setup for high-throughput small- and wide-angle solution scattering at the X33 beamline of EMBL Hamburg. Journal of Applied Crystallography 45 (2012) 0-0.

[20] P.V. Konarev, V.V. Volkov, A.V. Sokolova, M.H.J. Koch, D.I. Svergun, PRIMUS: a Windows PC-based system for small-angle scattering data analysis. Journal of Applied Crystallography 36 (2003) 1277-1282.

[21] A. Guinier, G. Fournet, C.B. Walker, K.L. Yudowitch, Small-angle scattering of X-rays, Wiley New York, 1955.

[22] D. Svergun, A direct indirect method of small-angle scattering data treatment. Journal of Applied Crystallography 26 (1993) 258-267.

[23] D. Svergun, Restoring low resolution structure of biological macromolecules from solution scattering using simulated annealing. Biophysical journal 76 (1999) 2879.

[24] R. Zoraghi, R.H. See, H. Gong, T. Lian, R. Swayze, B.B. Finlay, R.C. Brunham, W.R. McMaster, N.E. Reiner, Functional analysis, overexpression, and kinetic characterization of

pyruvate kinase from methicillin-resistant *Staphylococcus aureus*. Biochemistry 49 (2010) 7733-7747.

[25] G. Valentini, A. Mattevi, D. Barilla, A. Galizzi, M. Speranza, Recombinant pyruvate kinase type I from *Escherichia coli*: overproduction and revised C-terminus of the polypeptide. Biological chemistry 378 (1997) 719.

[26] E.R. Iliffe-Lee, G. McClarty, Pyruvate kinase from *Chlamydia trachomatis* is activated by fructose-2, 6-bisphosphate. Molecular microbiology 44 (2002) 819-828.

Legends to illustrations

Fig. 1: Expression and purification of PykA (A) and PykF (B). Coomassie-stained SDS-PAGE loaded with samples as indicated. BL21 pWS, whole cell lysate of expression host with backbone plasmid pWS treated with 0.1 mM IPTG; whole cell lysate of BL21 pWS-*pykA* and BL21 pWS-*pykF*, respectively, after induction with 0.1 mM IPTG; “soluble” and “insoluble” refer to soluble and insoluble fractions of the respective lysates after centrifugation; AIEC and GF represent pooled samples after anionic exchange chromatography and gel filtration chromatography, respectively.

Fig. 2: Structural characterization of PykA and PykF by CD spectroscopy. The far-UV spectra of PykA (22 µM), PykF (10 µM) and PykF + FBP (PykF: 9 µM; FBP: 10 mM) were recorded in 20 mM Tris-HCl (pH 8.0) at temperature 10 °C using a path length of 1 mm.

Fig. 3: SAXS-based low resolution structural models of PykA and PykF.

A: PykA; B: PykF; C: PykF + FBP.

Table 1

Summary of purification of *Yersinia enterocolitica* PykA recombinantly produced in *E. coli*[a]

Purification step	Total protein [mg]	PykA [mg]	Total activity [U/mg]	Specific activity [U/mg]	Purification [fold]	Purity [%]
Soluble bacterial lysate	321	112	15729	49	1	35
HiPrep 16/10 Q XL	128	109	11264	88	2.43	85
HiLoad 26/60 Superdex 200	105	100	8925	85	2.71	95

[a] From 400 ml of bacterial culture

Table 2

Summary of purification of *Yersinia enterocolitica* PykF recombinantly produced in *E. coli*[a]

Purification step	Total protein [mg]	PykF [mg]	Total activity [U/mg]	Specific activity [U/mg]	Purification [fold]	Purity [%]
Soluble bacterial lysate	275	124	9625	35	1	45
HiPrep 16/10 Q XL	98	88	9800	100	2	90
HiLoad 26/60 Superdex 200	79	73	8532	108	2.1	93

[a] From 400 ml of bacterial culture

Table 3

Comparison of published protocols on recombinant production of bacterial pyruvate kinases[a]

Organism and protein	Yield [mg/L]	Specific activity [U/mg]	Reference
Escherichia coli PykF	30	190	[25]
Staphylococcus aureus PK	30-40	100	[24]
Chlamydia trachomatis	6	55	[26]

[a]Only publications providing data on both yield and specific activity of recombinantly produced pyruvate kinases were included.

Hofmann *et al.*
Fig. 1

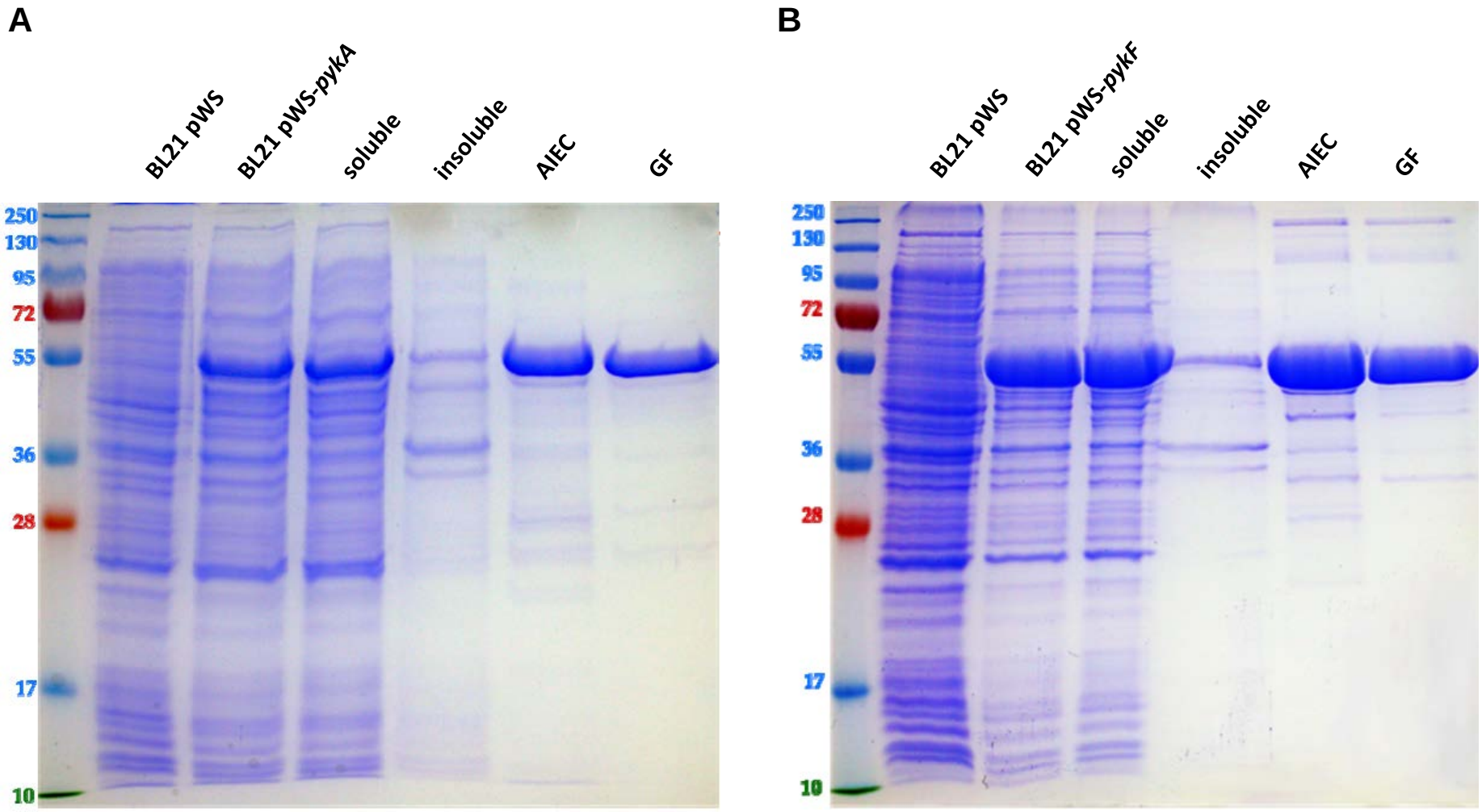

Hofmann *et al.*
Fig. 2

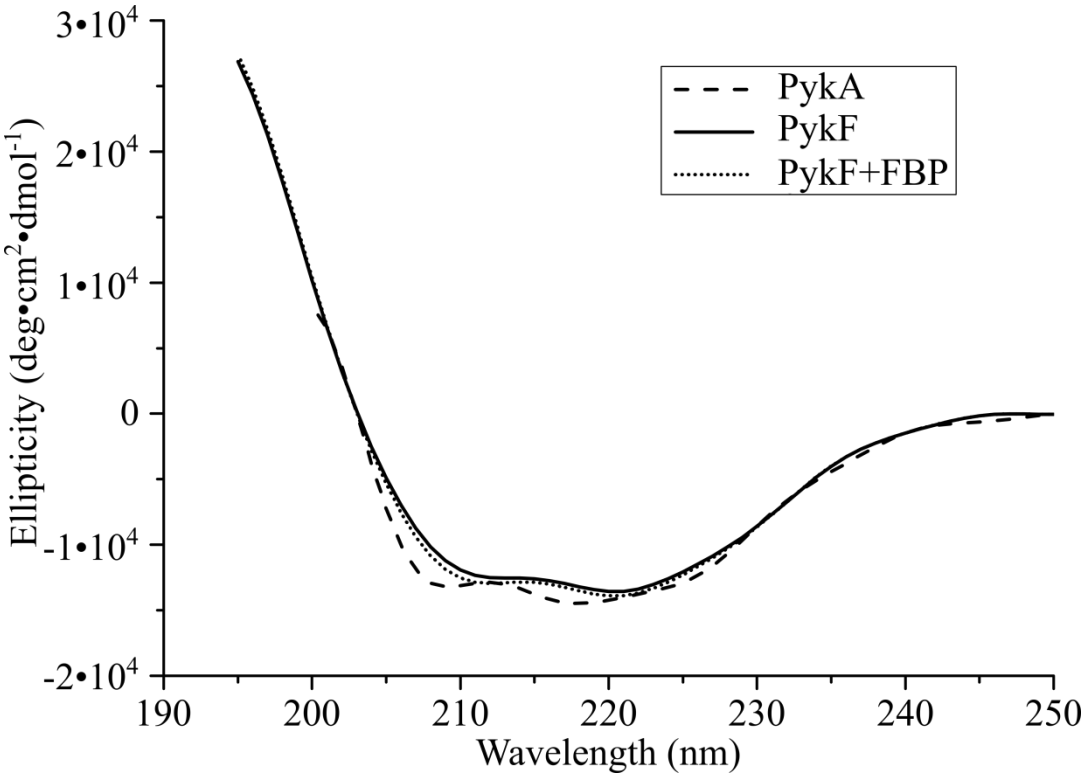

Hofmann *et al.*
Fig. 3

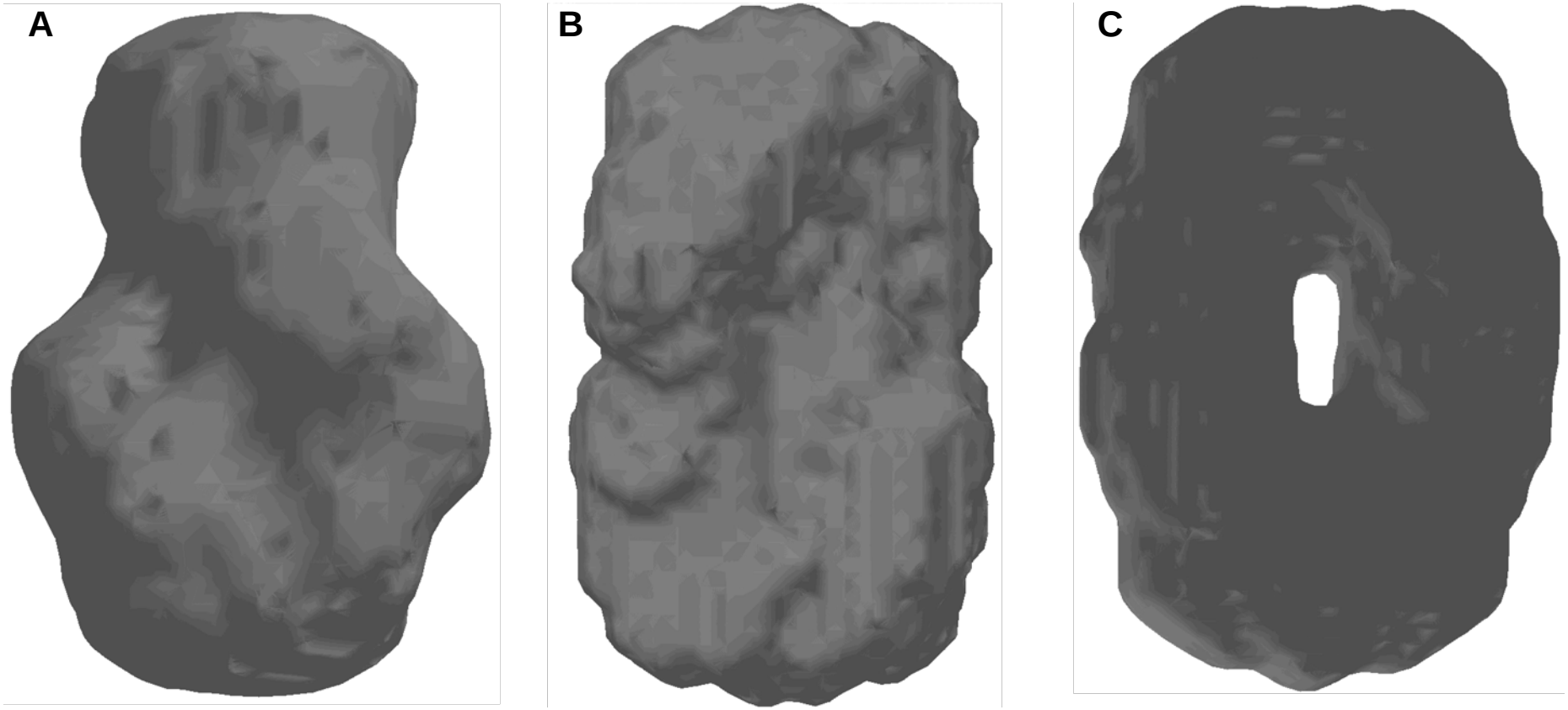

Hofmann *et al.*
Supplementary data 1

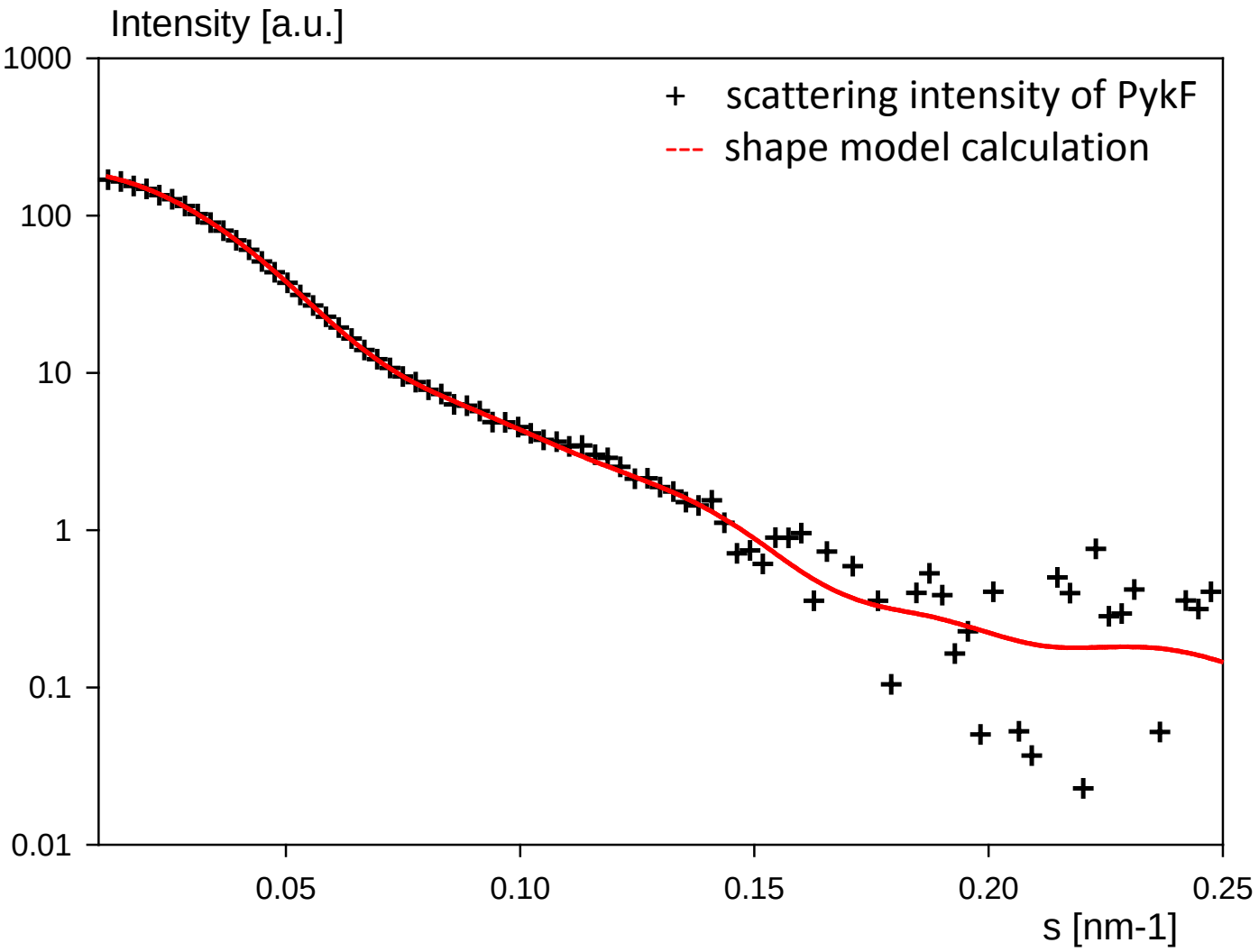

SAXS intensities of PykF in comparison with calculated shape model of PykF (Fig. 3). The chi value, describing the discrepancy of the experimental data to the shape model calculation is 1.1. The chi values for PykF+FBP and PykA (see Fig. 3) are similar.